Periodica Polytechnica
Mechanical Engineering

# Vibration and Noise of an Axial Flow Fan

59(3), pp. 109-113, 2015
DOI: 10.3311/PPme.7948


Tamás Kalmár-Nagy[1*], Bendegúz Dezső Bak[1],
Tamás Benedek[1], János Vad[1]

RESEARCH ARTICLE

Received 02 February 2015; accepted 18 March 2015

***Abstract***

*We describe a mechanical/acoustic study of a short-ducted axial flow fan. The purpose is to compare mechanical noise to that caused by flow phenomena.*

*The eigenfrequencies of the fan are identified through measurement and finite element computations. The fan acoustics is evaluated by beamforming studies using the Phased Array Microphone technique. The acoustic measurement data is processed by the Rotating Source Identifier method. The modal analysis of the fan model and the acoustic experiments reveal that the fan noise is dominated by mechanical noise in the few hundred Hz range and rotating sources of broadband noise above.*

***Keywords***

*Axial flow fan, vibration, noise, phased array microphone (PAM), ROSI algorithm*

[1] Department of Fluid Mechanics, Faculty of Mechanical Engineering, Budapest University of Techology and Economics, H-1111 Budapest, Bertalan L. Street 4-6, Hungary

[*] Corresponding author, e-mail: kalmarnagy@ara.bme.hu

## 1 Introduction

Characterizing aerodynamic and acoustic behavior of axial flow fans is a challenging problem. Not only are industrial fans often of controlled vortex design [1] operating at an off-design point, but due to the peculiarities of their configuration the noise emission may exceed the fan catalogue data.

A program to develop a simple method that provides design/re-design guidelines for less noise yet higher fan performance was initiated by Benedek, Vad, and Tóth [2, 3].

This paper presents the results of an investigation into the noise emitted by an axial industrial fan. Upstream noise emission from the fan is measured using a phased-array microphone (PAM) setup (a more detailed description of the PAM system and the beamforming algorithms can be found in [4]).

The beamforming (spatial filtering) methodology [5] creates maps of sound intensity based on the phase difference between the incoming acoustic signals at microphones. The resulting beamforming maps can be used to localize noise sources. Beamforming studies on axial flow turbomachines can distinguish between rotor-originated and other noise components [6], but these are usually laboratory tests, e.g. [7, 8, 9, 10, 11]. The classical frequency-domain based Delay & Sum algorithm [5]can localize standing sources, while the Rotating Source Identifier (ROSI) algorithm [6] can estimate the location of rotating sources.

Fan noise sources can be tonal (noise due to fan vibrations) and broadband. Broadband noise sources can be classified as [12, 13]:

(i) turbulence ingestion noise,
(ii) noise due to the interaction of the turbulent boundary layer with the blade surface,
(iii) trailing edge noise,
(iv) vortex shedding noise, due to the interaction of the boundary layers just downstream of the blade trailing edge,
(v) noise due to boundary layer separation.

Broadband noise source classes (ii) to (v) – termed altogether in [12] as “self-noise” – are determined by the condition of the blade boundary layers. The blade suction side of any rotor

blade, exposed to pronounced boundary layer growth, "faces" upstream. This suggest that in the "free-inlet" case (no upstream obstruction of the flow), the rotor noise radiated toward the upstream direction is dominated by rotor "self-noise". In addition to noise generation, the suction side boundary layer plays a major role also in generation of aerodynamic loss [14].

The structure of the paper is as follows. First, in Section 2 the fan geometry is characterized. Section 3 describes measurements and calculations of the eigenfrequencies of blade vibrations. Section 4 presents the acoustic measurements and Sections 5 and 6 discuss the results. Conclusions are drawn in Section 7.

## 2 Fan Geometry

The 1.8 kg fan [1] shown in Fig. 1 has $N$=5 circumferentially forward-skewed steel blades welded onto the hub. The blades are of circular-arc camber line with a thin profile of uniform thickness of 1 mm and of rounded leading and trailing edges. The hub houses the motor.

The following data were measured (using a ruler, a caliper and a Leica Racer 100 electric angle measurement device). Duct diameter is $d_p$=315 [mm] corresponding to a duct radius $r_p$=157.5 [mm]. The fan (tip) diameter is $d_t$=300 [mm], therefore the fan radius is $r$=150 [mm]. The hub diameter is $d_h$=94 [mm], therefore the hub radius is $r_h$=47 [mm]. The tip clearance was $g$=7.5 [mm] uniformly along the circumference.

Table 1 provides data on the blade geometry, including the chord $c$, curvature $f$, stagger angle γ and axis-normal sweep angle β˙ values at five nondimensionalised radii ($R$=$r/r_p$). $R$=0.30 corresponds to the hub radius, $R$=0.63 to the midspan radius and $R$=0.95 to the outermost blade radius (tip).

**Fig. 1** Axial flow fan: top view and side view

**Table 1** Blade geometry data

| $R$ [-] | $r$ [mm] | $c$ [mm] | $f$ [mm] | γ [°] | β˙ [°] |
|---|---|---|---|---|---|
| **0.30** | 47 | 88 | 12 | 35 | 0 |
| **0.46** | 73 | 97 | 9 | 33 | 23 |
| **0.63** | 99 | 108 | 9 | 31 | 31 |
| **0.79** | 124 | 118 | 8 | 29 | 39 |
| **0.95** | 150 | 130 | 8 | 27 | 44 |

## 3 Fan Vibrations

The vibration measurement device was a PCB 352C33 type piezoelectric accelerometer. The hub has a relatively high mass compared to one blade, therefore the accelerometer was placed to the top of the hub.

Five measurements were taken, each blade was hit once and the acceleration response was measured. The vibration spectrum (Fig. 2) was obtained via fast Fourier transformation. The differences between the results of the five independent measurements were negligible.

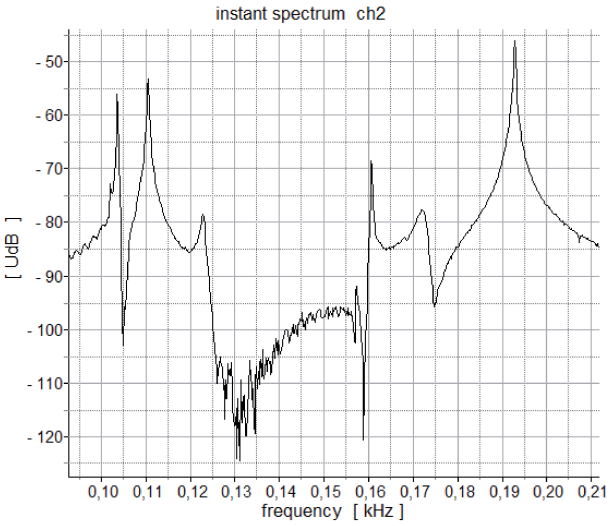


**Fig. 2** The frequency spectrum of the vibration

Groups of modes should contain five natural frequencies since the fan has five blades.

We note that it is difficult to distinguish frequencies that are close to one another. More measurements were taken changing the location of the excitation systematically to identify all relevant eigenfrequencies.

The first group of natural frequencies is located between 100 Hz and 125 Hz in the frequency domain.

The first ten natural frequencies are located in the range of 100 Hz and 200 Hz.

The measured frequencies are listed in Table 2.

**Table 2** Measurement and simulation results

| Measured Frequency [Hz] | Computed Frequency [Hz] |
|---|---|
| 101.5 | 104.6 |
| 103.8 | 104.6 |
| 110.5 | 112.5 |
| 123.0 | 126.3 |
| 125.1 | 126.3 |
| 156.6 | 156.6 |
| 160.4 | 156.8 |
| 167.4 | 166.9 |
| 171.6 | 167.1 |
| 192.7 | 189.5 |

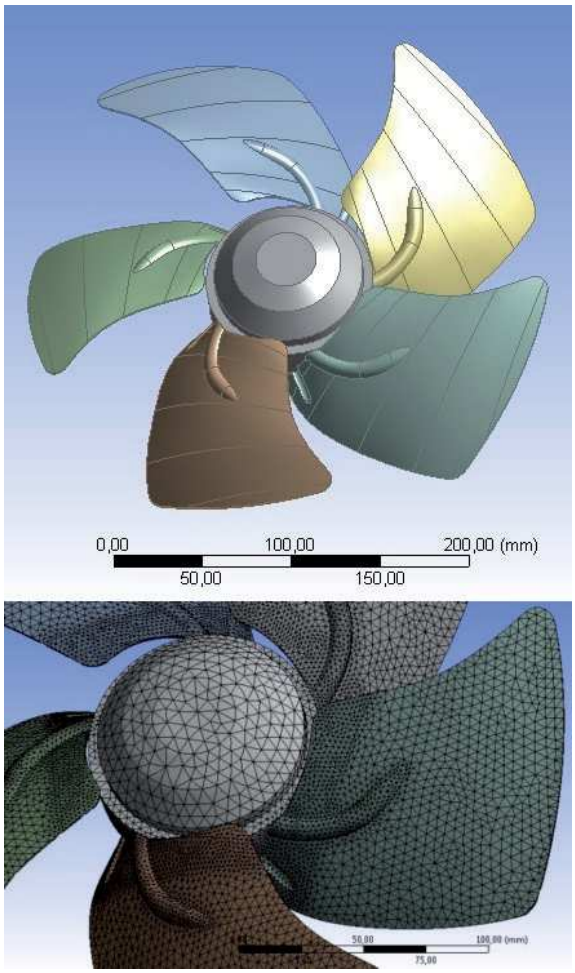


**Fig. 3** a) Ansys model of the fan, b) The meshed geometry

The fan was modeled using the Ansys Design Modeler [15] as can be seen in Fig. 3.

The steel blades (density of 7850 kg·m$^{-3}$) were modelled as surfaces with a given thickness and the hub as a solid, homogeneous body. Since the hub is actually a hollow body containing the motor, its average density is not known. The density of the hub was calculated such that the mass of the model and the actual mass of the fan matches, yielding 4300 kg·m$^{-3}$. For both the hub and blades we assumed a Young's modulus of 200 GPa.

The mesh consists of approximately 55500 elements. The maximum element side length is 10 mm. The element side lengths are refined to 2-4 mm over the blade surfaces and the connecting hub surfaces.

The fan has five blades in a symmetric, circular arrangement, therefore we expect 5 groups of equal frequencies (with some mistuning due to the coupling of blades through the hub).

The simulation results are listed in Table 2; the agreement between measured and computed eigenfrequencies is very good.

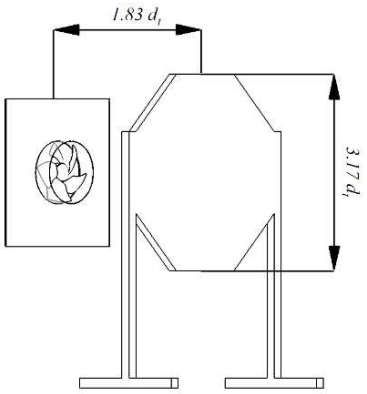


**Fig. 4** Measurement setup

## 4 Acoustic measurements

The noise signals were recorded using a general purpose Optinav Inc. 24-channel phased array microphone system (PAM, shown in Fig. 4). The microphones of the array are sunk into an octagonal aluminum plate, along a logarithmic spiral curve (this arrangement results in better sidelobe characteristics). The diameter of the circle enveloping the octagonal plate is 3.17 $d_t$ (fan diameter).

The microphone array was placed at a distance of 1.83 $d_t$ from the inlet plane of the fan casing. This distance enabled the detection of acoustic signals at a sufficiently high level but without overloading the microphones. Anemometer studies revealed that the impact of the PAM device on the flow field inlet to the fan is negligible.

The PAM (with its center coinciding with the rotor axis) was attached to an amplifier and to a sampler and analogue-to-digital converter. The rotor speed was measured by an optical tachometer.

The rotational speed of the fan is n=1430 rpm.

The acoustic data have been captured for 358 rotor revolutions (15 s) at a sampling frequency of 44.1 kHz.

## 5 Noise Spectrum

Figure 5 presents the acoustic spectrum calculated with Fast Fourier Transform from an individual microphone signal. The base frequency of the classic rotor-stator interaction noise is the blade passing frequency n*N (119 Hz) multiplied by the number of stator elements (2 pieces of fan supporting struts),

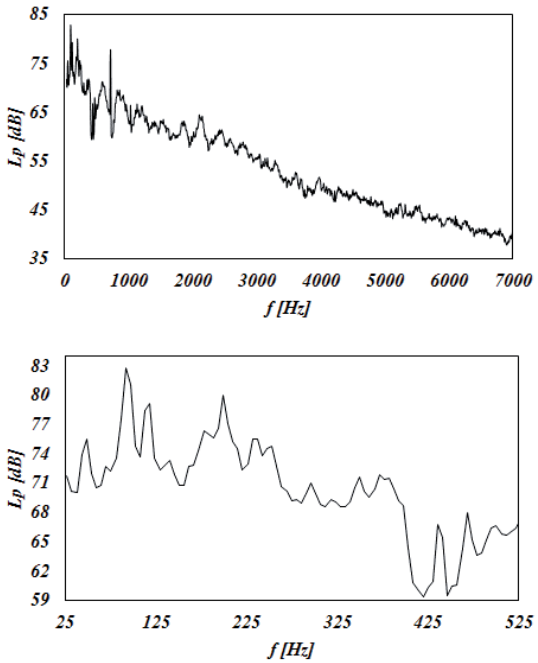


**Fig. 5** Acoustic spectra

being 238 Hz in this study. Although some peaks appear near 238 Hz and 2*238 Hz in the spectra associated with the fan, the spectrum indicates that mechanical fan noise dominates under 250 Hz while broadband noise is prevalent above 250 Hz.

## 6 Beamforming maps

The acoustic data were processed using the Acubeam software (written by Péter Tóth).

Figure 6 shows the beamforming maps, representing sound pressure in different frequency bands (the scales on the right-hand side correspond to values in dB). The maps correspond to an inspection area of 0.5 m*0.5 m, having the rotor in the center. The rotor annulus area is indicated in the maps using concentric circles (inner circle: at the hub of R = 0.30; outer circle: at the tip of R = 1.00).

Circles are presented on the top left corner of the maps in Fig. 6, the diameter of which corresponds to the estimated spatial resolution (the shortest distance within which two sources can be distinguished). This resolution is proportional to the distance between the sources and the array and is inversely proportional to the size of the array and to the frequency of interest [16]. Based on anechoic room measurements, the error has been estimated to be ±1.0 dB.

The maps for the third-octave band of $f_{mid}$ = 2500 and 3150 Hz confirm that the blades generate the most noise.

The ROSI noise source image patterns qualitatively show periodic variation of the sound pressure along the circumference at a given radius, especially at higher frequencies. This is due to the symmetry of the blade arrangement.

In the frequency bands belonging to $f_{mid}$ = 2500 and 3150 Hz, the near-midspan region is characterized by the most intense noise. The map related to $f_{mid}$ = 4000 Hz shows five

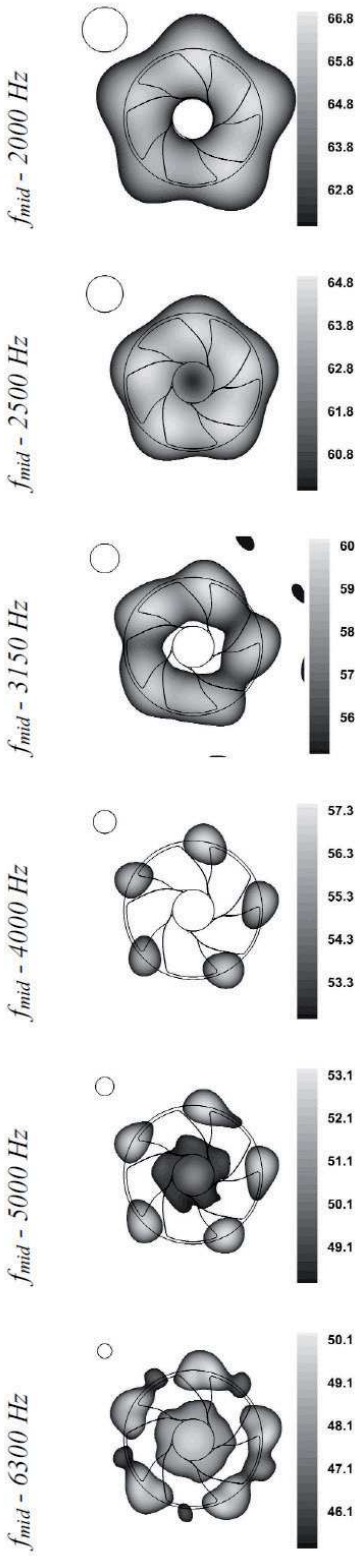


**Fig. 6** Beamforming maps. Scales on the right-hand side of the individual maps: $L_p$ values [dB]

local maxima of noise, related to the individual blades can be identified at a radius of R~0.85 (at ~80 percent span). Furthermore, extensive regions of increased noise can be detected, associated with the large suction surfaces of the blades.

On the maps related to $f_{mid}$ = 5000 and 6300 Hz, the noise of the electric motor, embedded in the hub, is comparable to

that of the blading. The source of maximum aero-acoustical noise is confined to the blade tip region. As one moves along the circumference of the casing, local maxima of noise can be associated with the individual blade passages. These can be attributed to tip leakage flow. This noise can be controlled by, for example, means of passive noise control [17].

## 7 Conclusion

We describe the investigation of mechanical and flow-induced fan noise. Upstream noise emission was measured using a phased-array microphone setup and evaluated by creating sound intensity maps. The eigenfrequencies of the fan were identified through measurement and finite element computations. The modal analysis of the fan model and the acoustic experiments reveal that the fan noise is dominated by mechanical noise in the few hundred Hz range and rotating sources of broadband noise above.


## Acknowledgement

This work has been supported by the Hungarian National Fund for Science and Research under contract No. OTKA K 112277. Gratitude is expressed to Mr. Bence TÓTH for carrying out the geometrical measurements, to Mr. István DÁNIEL for his help in the vibration measurements.

The work relates to the scientific program of the project "Development of quality-oriented and harmonized R+D+I strategy and the functional model at BME", supported by the New Hungary Development Plan (Project ID: TÁMOP-4.2.1/B-09/1/KMR-2010-0002). It is also supported by the project "Talent care and cultivation in the scientific workshops of BME" project (Project ID: TÁMOP-4.2.2/B-10/1-2010-0009).


## References


[1] Vad, J. "Forward Blade Sweep Applied to Low-Speed Axial Fan Rotors of Controlled Vortex Design: An Overview." *ASME Journal of Engineering for Gas Turbines and Power.* 135 (1). pp. 1-9. 2013. DOI: 10.1115/1.4007428

[2] Benedek, T., Vad, J. "Concerted Aerodynamic and Acoustic Diagnostics of an Axial Flow Industrial Fan, Involving the Phased Array Microphone Technique." In: *ASME Turbo Expo 2014: Turbine Technical Conference and Exposition*. Düsseldorf. 2014. DOI: 10.1115/GT2014-25916

[3] Tóth, B. "*Phased Array Microphone Measurement of an Axial Flow Fan*." Budapest: BME Department of Fluid Mechanics. 2014.

[4] Benedek, T., Tóth, P. "Beamforming Measurements of an Axial Flow Fan in an Industrial Environment." *Periodica Polytechnica Mechanical Engineering.* 57 (2). pp. 37-46. 2012. DOI: 10.3311/PPme.7043

[5] Underbink, J. R. "Aeroacoustic Phased Array Testing in Low Speed Wind Tunnels." In: Mueller, T. J. (ed.) *Aeroacoustic Measurements*. London: Springer. 2002. DOI: 10.1007/978-3-662-05058-3_3

[6] Sijtsma, P., Oerlemens, S., Holthusen, H. "Location of Rotating Sources by Phased Array Measurements." *AIAA Paper 2167-2001*. 2001. DOI: 10.2514/6.2001-2167

[7] Lowis, C., Joseph, P. "Determining the Strength of Rotating Broadband Sources in Ducts by Inverse Methods." *Journal of Sound and Vibration.* 295 (3-5). pp. 614-632. 2005. DOI: 10.1016/j.jsv.2006.01.031

[8] Sijstma, P. "Using Phased Array Beamforming to Identify Broadband Noise Sources in a Turbofan Engine." *International Journal of Aeroacoustics.* 9 (3). pp. 357-374. 2010. DOI: 10.1260/1475-472x.9.3.357

[9] Minck, O., Binder, N., Cherrier, O., Lamotte, L. Budinger, V. "Fan Noise Analysis Using a Microphone Array." In: *Proceedings International Conference on Fan Noise.* Senlis, 2012.

[10] Podboy, G. G., Horváth, C. "Phased Array Noise Source Localization Measurements Made on a Williams International FJ44 Engine." *AIAA Paper 2009-3183.* 2009. DOI: 10.2514/6.2009-3183

[11] Horváth, C., Podboy, G. G., Envia, E. "Limitations of Phased Array Beamforming in Open Rotor Noise Source Imaging." *AIAA Paper 2013-2098.* 2013.

[12] Carolus, T. "*Ventilatoren*." Teubner Verlag. 2003.

[13] De Gennaro, M., Kuenhelt, H. "Broadband Noise Modelling and Prediction for Axial Fans." In: *Proceedings International Conference on Fan Noise.* Senlis. 2012.

[14] Vad, J. "Correlation of Flow Path Length to Total Pressure Loss in Diffuser Flows." *IMechE, Part A - Journal of Power Energy.* 225 (4). pp. 481-496. 2011. DOI: 10.1177/0957650910397113

[15] "Design Modeler User's Guide, Ansys Help viewer, Version 15.0." Ansys Inc. 2013.

[16] Hald, J. "Combined NAH and Beamforming Using the Same Array." Brüel & Kjaer Technical Note. 2005.

[17] Bianchi, S., Corsini, A., Rispoli, F., Sheard, A. G. "Experimental Aeroacoustic Studies on Improved Tip Configurations for Passive Control of Noise Signatures in Low-Speed Axial Fans." *ASME Journal of Vibration and Acoustics.* 131 (6). pp. 1-10. 2009. DOI: 10.1115/1.4000462